Tonic GluD1 channel current is independent of G protein activity in the dorsal raphe nucleus

Daniel S. Copeland[1] and Stephanie C. Gantz[1]

Affiliations: Department of Molecular Physiology and Biophysics, University of Iowa, Iowa City, IA, 52242, USA

Corresponding author: Stephanie-Gantz@uiowa.edu

ABSTRACT

Previously, using electrophysiological recordings from adult male and female mouse brain slices containing the dorsal raphe nucleus, we showed that GluD1$_R$ channels carry ionic current and are modulated via activation of Gα_q-coupled α1-adrenergic receptors (α1-A$_R$) in a GTP-dependent manner (Gantz et al., 2020). GluD1$_R$ channels also carry a tonic cation current, generally ~-20 pA at subthreshold membrane potentials (Gantz et al., 2020). The origin of tonic GluD1$_R$ channel current is unknown. Here, using the same preparation, we show there is no role of on-going G protein-coupled receptor activity in generating or sustaining tonic GluD1$_R$ channel current. Neither augmentation nor disruption of G protein activity had an effect on tonic GluD1$_R$ current. These results reveal that tonic GluD1$_R$ current arises from a mechanism separate from on-going activity of G protein-coupled receptors. Under current clamp, block of GluD1$_R$ channels hyperpolarized the membrane by ~10 mV at subthreshold potentials leading to reduced excitability. Thus, GluD1$_R$ channels carry a G protein-independent tonic current that contributes to subthreshold drive of action potential firing in the dorsal raphe nucleus.

INTRODUCTION

The majority of excitatory neurotransmission in the central nervous system is produced by ionic current carried by the ionotropic glutamate receptors (iGluRs). Lesser known in the iGluR family are the delta glutamate receptors (GluD1$_R$ and GluD2$_R$) which share <30% amino acid sequence identity with the other family members (Araki et al., 1993; Lomeli et al., 1993). GluD1$_R$ are expressed widely in the brain (Hepp et al., 2015; Konno et al., 2014; Nakamoto et al., 2020), where they regulate inhibitory and excitatory synapse formation and composition in complex with trans-synaptic and secreted proteins (Dai et al., 2021; Fossati et al., 2019; Gawande et al., 2021; Tao et al., 2018). These functions do not involve ion conduction through the channel pore (reviewed in Yuzaki and Aricescu, 2017). The study of ion channel function of GluD1$_R$ has been limited since there is no known agonist that binds to GluD1$_R$ directly to gate opening of the channel. Nonetheless, we and others have demonstrated that GluD1$_R$ and GluD2$_R$ channels carry ionic current upon activation of Gα_q protein-coupled receptors (GqPCRs), either metabotropic glutamate (mGlu$_R$, Ady et al., 2013; Benamer et al., 2018; Dadak et al., 2017) or α1-adrenergic

receptors (Gantz et al., 2020), through a process that involves intact G protein signaling. Intriguingly, in cell lines and brain slices, $GluD1_R$ and $GluD2_R$ channels are open in the presumed absence of agonists and carry tonic cation current (Gantz et al., 2020; Lemoine et al., 2020). The origin of the tonic $GluD_R$ current is unknown.

Typically, GPCRs are activated when extracellular ligands bind to the receptor and force a conformational change which initiates downstream signal transduction mechanisms. In principle, GqPCRs could exhibit low levels of activation in response to ambient ligand, as demonstrated recently for $G\alpha_{i/o}$ protein-coupled dopamine D2 receptors (Rodriguez-Contreras et al., 2021). GPCRs can also be constitutively active; entering an active state conformation in the absence of ligand (reviewed in Bond and IJzerman, 2006). Despite knowledge that $GluD1_R$ channels are modulated by a GTP-dependent mechanism (Gantz et al., 2020) whether the tonic $GluD1_R$ current is a product of low-level GqPCR activity is not established.

Here, using patch-clamp electrophysiology in acute mouse brain slices containing the dorsal raphe nucleus, we show that manipulating G protein activity did not impact the amplitude of the tonic $GluD1_R$ current. Augmentation of on-going G protein activity amplified tonic potassium current carried by G protein-coupled inwardly rectifying potassium (GIRK) channels, but not tonic $GluD1_R$ current. Inverse agonism of α1-adrenergic receptors did not affect the tonic $GluD1_R$ current, suggesting a key modulator of $GluD1_R$ channel current is not responsible for generating tonic $GluD1_R$ current. Further, depletion of cell-autonomous G protein activity did not change the amplitude of the tonic $GluD1_R$ current. Thus, tonic $GluD1_R$ current arises from a mechanism separate from on-going, cell-autonomous GPCR activity.

Results and Discussion

$GluD1_R$ channels carry a tonic current

Whole-cell voltage-clamp recordings were made from dorsal raphe neurons in acute brain slices from wild type mice at 35° C in the presence of $NMDA_R$, $AMPA_R$, and $kainate_R$ blockers, using a potassium-based internal solution (V_{hold} -65 mV). Our previous work showed that $GluD1_R$ channels carry an ~-20 pA tonic current, revealed by the application of a channel blocker, 1-naphthyl acetyl spermine (NASPM) and by genetic deletion of the $GluD1_R$

channel (Gantz et al., 2020). In agreement with our prior work, here we show that application of NASPM (100 μM) produced an apparent outward current of 18.2±2.8 pA ($p = 0.02$, $n = 7$, Figures 1A and B). On average, the current peaked in 3.5 min and reversed in 11 min upon washout of NASPM. The outward current was accompanied by an increase in the membrane resistance ($p = 0.02$, $n = 7$, Figure 1C) and a reduction in the membrane noise variance (σ^2, $p = 0.02$, $n = 7$, Figure 1D), indicating fewer open channels. NASPM failed to change the current when external Na^+ (126 mM) was replaced with N-methyl D-glucamine (-3.0±3.6 pA, $p = 0.50$, $n = 3$). In all, these findings reproduce those of our previous work (Gantz et al., 2020) and demonstrate that NASPM blocks a tonic, sodium-dependent inward current.

Tonic GluD1$_R$ current is not produced by G protein activity

GluD1$_R$ and GluD2$_R$ channels carry ionic current following the activation of either mGlu$_R$ or α1-adrenergic receptors (Ady et al., 2013; Benamer et al., 2018; Dadak et al., 2017; Gantz et al., 2020; Lemoine et al., 2020). GluD2$_R$ current, seen upon mGlu$_R$1 activation in cell lines, is dependent on canonical GqPCR signaling as the agonist-induced current is blocked by bath application of G$\alpha_{q/11}$ or phospholipase C inhibitors (Dadak et al., 2017). Similarly, GluD1$_R$ ionic current activated by α1-adrenergic receptors in dorsal raphe neurons is abolished after internal dialysis with GDPβS-Li_3 (Gantz et al., 2020), a non-specific disruptor of G protein activity and other processes requiring a GDP-GTP exchange. Following our original report of tonic GluD1$_R$ current in brain slices (Gantz et al., 2020), Lemoine et al., (2020) reported a very similar tonic current carried by GluD2$_R$ channels when expressed in cell lines with mGlu$_R$1. mGlu$_R$, like many GPCRs, can exhibit constitutive activity in the absence of agonist (Prézeau et al., 1996) and low-level constitutive activity of GPCRs affects other subthreshold cation conductances (Lu et al., 2010; Philippart and Khaliq, 2018; Quallo et al., 2017; Shen et al., 2012; Zhang et al., 2012). But, the involvement of GqPCRs in generating tonic GluD1$_R$ current has not been explored.

To test whether increased G protein activity was sufficient for generating tonic GluD1$_R$ current, the internal recording solution was supplemented with a non-hydrolyzable GTP analog (guanosine-5'-[(β, γ)-imido]triphosphate, GppNHp, 1 mM), which binds irreversibly to Gα and elevates G protein activity. In dorsal raphe

neurons, dialysis with GppNHp produces a tonic outward current carried by G protein-coupled inwardly rectifying potassium (GIRK) channels (Loucif et al., 2006) by elevating free Gβγ subunits which gate GIRK channels (Pfaffinger et al., 1985). In agreement, whole-cell dialysis of GppNHp-containing internal solution (≥10 min) produced a tonic outward current with a reversal potential of -108 mV (Figures 2A and B), consistent with the expected reversal potential of potassium (calculated E_K: -104 mV). Application of $BaCl_2$ (100 μM), which blocks GIRK channels (Gantz et al., 2013) produced an apparent inward current (-46.0±10.6 pA, Figure 2A) with GppNHp- but not GTP-containing internal solution (p = 0.0003, n = 9-16, Figure 2C). These data demonstrate that amplifying G protein signaling with GppNHp produces standing currents carried by G protein-gated ion channels, consistent with previous studies (Kramer and Williams, 2016; Loucif et al., 2006). In the continued presence of $BaCl_2$, tonic $GluD1_R$ current was measured following application of NASPM (Figure 2D). On average, tonic $GluD1_R$ current was -16.7±2.8 pA, which was not different from current measured with GTP-containing internal solution (p = 0.72, n = 5-8, Figure 2E). $BaCl_2$ had no effect on the amplitude of the α1-adrenergic receptor-dependent excitatory postsynaptic current (ctrl: -20.6±3.6 pA; $BaCl_2$: -26.0±4.1 pA, p = 0.20, n = 8), evoked by electrical stimulation of the brain slice (5 pulses, 0.5 ms, 60 Hz) delivered via a monopolar stimulating electrode, indicating that at this concentration, external $BaCl_2$ does not affect conductance of $GluD1_R$ channels. Taken together, the data suggest that augmenting G protein activity has a negligible impact on the amplitude of the tonic current carried by $GluD1_R$ channels.

In principle, GPCRs could be activated by ambient ligand in brain slices to produce a small tonic current. In midbrain dopamine neurons, ambient activation of $G\alpha_{i/o}$-coupled dopamine D2 receptors produces a tonic GIRK current of ~9 pA (Rodriguez-Contreras et al., 2021). Next, we tested whether tonic $GluD1_R$ current was dependent on α1-adrenergic receptor activity, either from ambient ligand or constitutive activity, by applying an α1-adrenergic receptor inverse agonist prazosin (100 nM, Hein et al., 2001). Prazosin had no effect on the magnitude of the tonic $GluD1_R$ current (-21.2±2.8 pA, p = 0.22, n = 5). In midbrain dopamine neurons, $GluD1_R$ channel current is produced by activation of $mGlu_R$ (Benamer et al., 2018), suggesting a similar mechanism may occur in the dorsal raphe. Moreover, in the dorsal raphe, $G\alpha_q$-coupled histamine H_1 and orexin OX_2 receptors converge on the same

downstream effectors as α1-adrenergic receptors (Brown et al., 2002), suggesting if the tonic GluD1$_R$ current was produced via G protein activity, there are many types of receptors to consider. As a broad test as to whether tonic GluD1$_R$ current was dependent on G protein signaling, recordings were made with an internal solution where GTP was replaced with a non-hydrolyzable analog of GDP, GDPβS-Li$_3$ (1.24 mM) which acts as a competitive antagonist at GTP-binding sites. Within 10 mins of whole-cell dialysis with GDPβS-containing internal solution, application of noradrenaline (30 μM) produced an inward GluD1$_R$ current (Figures 3A and B). By ≥20 min of whole-cell dialysis, the noradrenaline-induced current was abolished ($p = 0.02$, $n = 7$, Figures 3A and B), confirming efficacy of GDPβS to arrest α1-adrenergic receptor-GluD1$_R$ channel signaling (Gantz et al., 2020). In contrast, GDPβS had no effect on the tonic GluD1$_R$ current when compared with GTP-containing internal solution with or without a similar concentration of LiCl (GDPβS-Li$_3$: -28.7±4.9 pA, $n = 13$, GTP: -19.3±2.7 pA, GTP + LiCl: -23.5±3.9 pA, $n = 8$-13, $p = 0.46$, Figure 3C). Further, there was no decrement in the magnitude of the tonic GluD1$_R$ current with repeat applications of NASPM ($p = 0.84$, $n = 6$, Figures 3D and E). Taken together, these results demonstrate that tonic GluD1$_R$ current is independent of cell-autonomous G protein signaling.

Tonic GluD1$_R$ current provides subthreshold drive of action potential firing

Throughout the central nervous system, many types of neurons fire action potentials in a rhythmic 'pacemaker' pattern. Some are autonomous pacemakers, driven by intrinsic membrane properties, while others are conditional pacemakers that rely on synaptic input and receptor stimulation. A common feature in autonomous pacemakers is the presence of a tonic, subthreshold, tetrodotoxin-insensitive, cation/sodium current (Eggermann et al., 2011; Jackson et al., 2004; Khaliq and Bean, 2010; Li et al., 2021; Lu et al., 2007; Raman et al., 2000). While many different types of channels are involved, these tonic currents each function to depolarize the membrane to ~- 60 mV where voltage-dependent mechanisms of action potential firing are engaged. Primarily, serotonin neurons are conditional pacemakers and require subthreshold drive from noradrenergic afferents and activation of α1-adrenergic receptors (Baraban et al., 1978; Vandermaelen and Aghajanian, 1983) much like other conditional pacemakers which require activation of Gα_q-coupled orexin or muscarine receptors (Egorov et al., 2019, 2002; Top et al., 2004;

Yamada-Hanff and Bean, 2013). In these neurons, activation of GqPCRs leads to subthreshold (~-70 to -55 mV) depolarization via a very similar cation current as the tonic current observed in autonomous pacemakers. While these tonic cation currents are essential for subthreshold depolarization, it is not unusual for the current to be quite small, only a few to tens of picoamperes (Jackson et al., 2004; Raman et al., 2000; Taddese and Bean, 2002).

To determine if tonic $GluD1_R$ current contributed to subthreshold excitation, whole-cell current clamp recordings were made from dorsal raphe neurons and APs were evoked with somatic current injection (1.5 s, 20 pA increments, Figure 4A). In the absence of noradrenaline, dorsal raphe neurons are silent or fire slowly and erratically (Baraban et al., 1978; Svensson et al., 1975). Consistent with the absence of ambient noradrenaline in brain slices, 5/10 neurons were firing spontaneously at a slow and irregular rate (0.8±0.3 Hz) and 5/10 only fired in response to current injection. After application of NASPM (30 – 50 μM), 1/10 neurons fired spontaneously, and the rest became quiescent until APs were evoked by current injection (Figure 4B). At subthreshold potentials (-80 to -55 mV), NASPM hyperpolarized the membrane by ~10 mV (Figure 4C), consistent with expectations given the magnitude of the tonic $GluD1_R$ current (-19.6±4.0 pA) and basal membrane resistance (555.6±45.4 MΩs). Consequently, NASPM increased the minimum current necessary to evoke AP firing (approximate rheobase), which reversed upon 10 min washout of NASPM ($p = 0.005$, n = 4-9, Figure 4D) and increased the latency to fire the first AP ($p = 0.02$, Figure 4E). In contrast, once the membrane reached threshold, NASPM had little-to-no effect on average membrane potential between APs (Figure 4C). The AP waveform was largely unaffected by NASPM (Figure 4F), consistent with a reversal potential of ~-30 mV and intrinsic inward rectification (Gantz et al., 2020). However, it should be noted that NASPM preferentially blocks inward flow and strong depolarization relieves pore block (Koike et al., 1997). Thus, observation of any contribution of outward ion flux may be obscured. There were no differences in the AP half-width ($p=0.19$), after-hyperpolarization ($p = 0.38$), height ($p = 0.06$), or threshold ($p > 0.99$, Figure 4G). But there was a significant decrease in the slope of the voltage trajectory between APs ($p = 0.02$, Figures 4F and H), resulting in a delay to the next AP (interspike interval, $p = 0.04$, Figure 4I). Overall, NASPM reduced AP firing frequency ($p = 0.01$, two-way ANOVA, measured from the first 3 APs, Figure 4J). Thus, tonic $GluD1_R$ current contributes to subthreshold drive of action potential firing. Provided the widespread distribution in

the brain (Hepp et al., 2015; Konno et al., 2014; Nakamoto et al., 2020), $GluD1_R$ channels may contribute to pacemaking in other neuronal populations, whether via intrinsic tonic current or following GqPCR activation. Future work will be needed to determine whether tonic $GluD1_R$ current arises from an intrinsic property of the channel (i.e. an open *apo*-state) or is generated by an unidentified ligand.

Methods

Animals

All studies were conducted in accordance with the University of Iowa with the approval of the University of Iowa Institutional Animal Care and Use Committee. Male and female wild type C57BL/6J (>2 months old, The Jackson Laboratory, #000664) mice were used. Mice were group-housed on a 12:12 h light cycle.

Brain slice preparation and electrophysiological recordings

Brain slices and electrophysiological recordings were made as previously described (Khamma et al., 2021). In brief, mice were deeply anesthetized with isoflurane and euthanized by decapitation. Brains were removed and placed in warmed and bubbled (95/5% O_2/CO_2) modified Krebs' buffer containing (in mM): 126 NaCl, 2.5 KCl, 1.2 $MgCl_2$, 1.2 $CaCl_2$, 1.2 NaH_2PO_4, 21.5 $NaHCO_3$, and 11 D-glucose with 5 μM MK-801 to reduce excitotoxicity and increase slice viability. In the same solution, coronal dorsal raphe slices (240 μm) were obtained using a vibrating microtome (Leica 1220S) and incubated at 28 °C >30 minutes prior to recording.

Electrophysiological recordings were made in NBQX (3 μM) solutions at 35 °C with Multiclamp 700B amplifiers (Molecular Devices), Digidata 1440A and 1550B A/D converters (Molecular Devices), and Clampex software (Molecular Devices) with borosilicate glass electrodes (World Precision Instruments) wrapped with Parafilm to reduce pipette capacitance. Pipette resistances were 3.8 to 4.5 MΩ when filled with an internal solution containing, (in mM) 104.56 K-methylsulfate, 3.73 KCl, 5.3 NaCl, 4.06 $MgCl_2$, 4.06 $CaCl_2$, 7.07 HEPES (K), 3.25 BAPTA (K4), 0.26 GTP (sodium salt), 4.87 ATP (sodium salt), 4.59 creatine phosphate (sodium salt), pH 7.24 with KOH, mOsm ~274, for whole-cell patch-clamp recordings. Series resistance was monitored throughout the experiment. Reported

184 voltages are corrected for a liquid junction potential of -8 mV between the internal and external solution. All drugs
185 were applied via the patch-pipette or by bath application. Noradrenaline was applied in the presence of an α2-
186 adrenergic antagonist, idazoxan (1 μM).
187
188 *Materials*
189 $BaCl_2$: Sigma, 217565
190 GDPβS-Li_3: Sigma, G7637
191 GppNHp: Sigma, G0635
192 Idazoxan: Sigma, I6138
193 LiCl: Sigma, L4408
194 MK801: Tocris, 0924
195 NASPM: Tocris, 2766
196 NBQX: Tocris, 1044
197 NMDG: Sigma, M2004
198 Noradrenaline: Tocris, 5169
199 Prazosin: Tocris, 623
200 Igor-Pro 6.37: Wavemetrics
201 DataAccess: Bruxton Corporation
202 Clampfit 10.7: Molecular Devices
203 GraphPad Prism 8.4.3: GraphPad Software
204
205 *Experimental Design and Statistical Analysis*
206 Data were analyzed using Clampfit 10.7 or Igor-Pro 6.37 software, and are presented in representative traces,
207 scatter plots and bar graphs with means ± SEM. Unless otherwise noted, *n* = number of cells as biological replicates.
208 Tonic current was measured as the peak of the NASPM-induced current minus the whole-cell current prior to

NASPM application. Reversal potentials were determined using linear fit of the averaged data accounting for scatter amongst the replicates using five data points above and below where the current reversed polarity. Significant differences were determined via Wilcoxon matched-pairs signed rank tests for within-group comparisons, and Mann Whitney tests for between-group comparisons. A difference of $p<0.05$ was considered significant. Exact values are reported unless $p<0.0001$ or >0.999. Statistical analysis was performed using GraphPad Prism 8.4 (GraphPad Software, Inc.).

Acknowledgements

This research was funded by a startup award from the University of Iowa Carver College of Medicine to S.C.G. We thank Holly S. Hake for critical reading and comments on the manuscript.

Author Contributions

Conceptualization, S.C.G., experimental setup and development, D.S.C. and S.C.G.; experiments, D.S.C. and S.C.G.; analysis, D.S.C. and S.C.G.; writing & editing, D.S.C. and S.C.G.

Conflict of interest: The authors declare no competing interests.

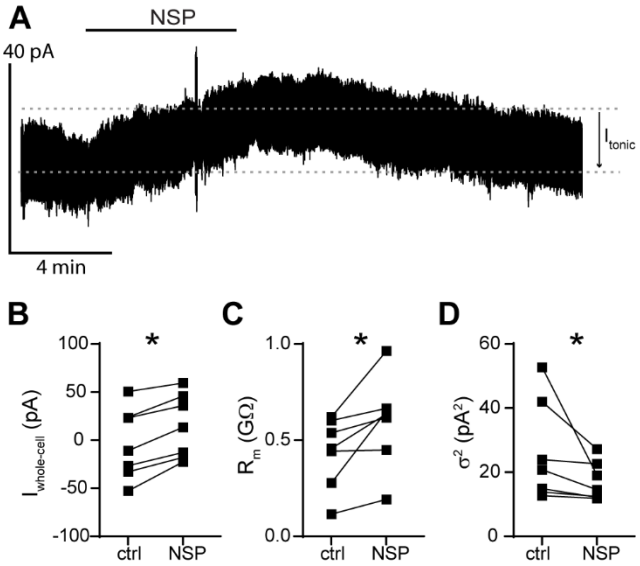

Figure 1. NASPM reveals a tonic inward current carried by GluD1$_R$ channels. (**A**) Representative whole-cell voltage-clamp recording of the apparent outward current produced by application of NASPM (NSP, 100 μM). Dashed lines indicate baseline current (bottom) and the peak of the outward current (top). Tonic current was measured as the difference of these lines ($I_{tonic,}$ arrow). (**B**) Plot of the whole-cell current (V_{hold} -65 mV) in control conditions (ctrl) and after application of NASPM (NSP, p = 0.016, n = 7). (**C**) Plot of basal membrane resistance recorded in control conditions (ctrl) and during NASPM application (NSP p = 0.016, n = 7). (**D**) Plot of membrane noise variance (σ^2) in control conditions (ctrl) and during NASPM application (NSP, p = 0.016, n = 7). Line and error bars represent mean ± SEM. * denotes statistical significance.

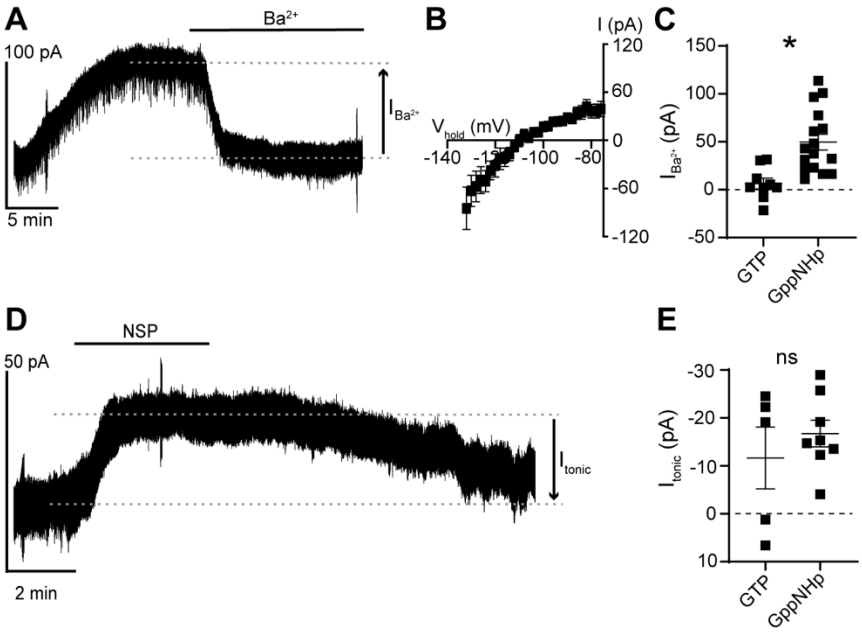

Figure 2. Augmentation of G protein activity with GppNHp has no effect on the tonic current carried by GluD1$_R$. (**A**) GppNHp-containing internal solution produced a tonic Ba^{2+}-sensitive (100 μM) outward current, shown in a representative whole-cell voltage-clamp recording. (**B**) Current-voltage relationship of the tonic Ba^{2+}-sensitive (100 μM) outward current demonstrating reversal near expected E_K and inward rectification. (**C**) Plot of tonic GIRK currents measured in control conditions (GTP) and with GppNHp-containing internal solution ($p = 0.0003$, $n = 9$ and 16 respectively). (**D**) GppNHp had no effect on the NASPM (NSP, 100 μM)-sensitive inward current, shown in a representative recording. (**E**) Plot of the magnitude of GluD1$_R$ tonic current measured with GTP-containing internal solution as compared to GppNHp-containing internal solution ($p = 0.72$, $n = 5$ and 8 respectively) when measured in external Ba^{2+} to block tonic GIRK current. Line and error bars represent mean ± SEM. * denotes statistical significance, ns denotes not significant.

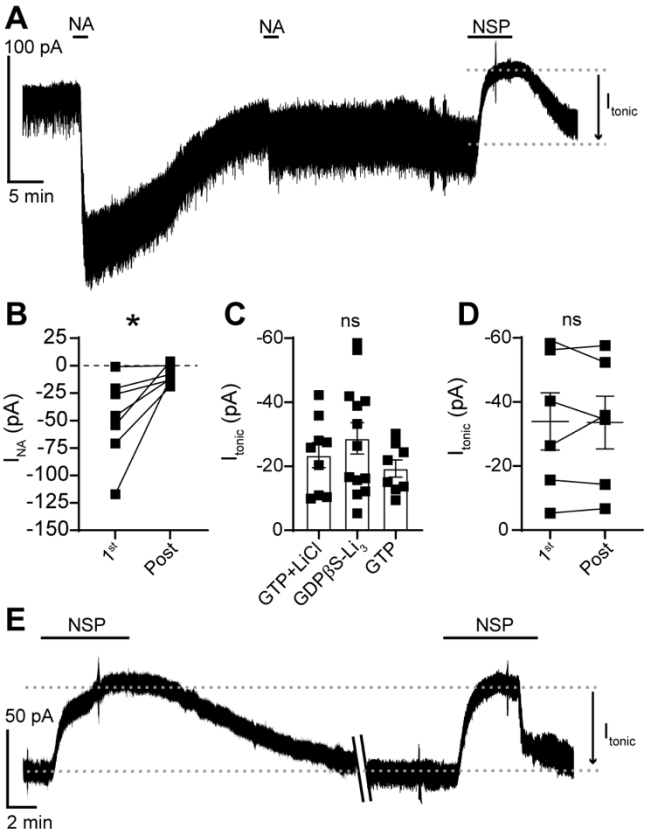

Figure 3. The GluD1$_R$ tonic current is not dependent on G protein signaling. (**A**) With GDPβS-containing internal solution, noradrenaline-induced GluD1$_R$ current (I_{NA}) was diminished by >20 minutes post-dialysis, shown in a representative trace. (**B**) With GDPβS-containing internal solution, the amplitude of I_{NA} ran down with whole-cell dialysis; shown in a plot of the first application of noradrenaline (30 μM, 1st) compared to application of noradrenaline >20 min post-dialysis (Post, p = 0.02, n = 7). (**C**) Plot of I_{tonic} measured after dialysis with GTP + LiCl-, GDPβS-Li_3-, and GTP-containing internal solution, displaying no significant difference between the groups (p = 0.46, n = 9, 13, 8 respectively). (**D**) Plot of I_{tonic} recorded with GDPβS-containing internal solution for the first application of NASPM (1st) and application of NASPM >45 min post-dialysis, showing no difference in the average amplitude (Post, p = 0.84, n = 6). (**E**) With GDPβS-containing internal solution, repeated application of NASPM revealed tonic GluD1$_R$ current without a decrement in amplitude, shown in a representative trace. Slanted lines indicate a 40-minute wash time in the recording. Line and error bars represent mean ± SEM. * denotes statistical significance, ns denotes not significant.

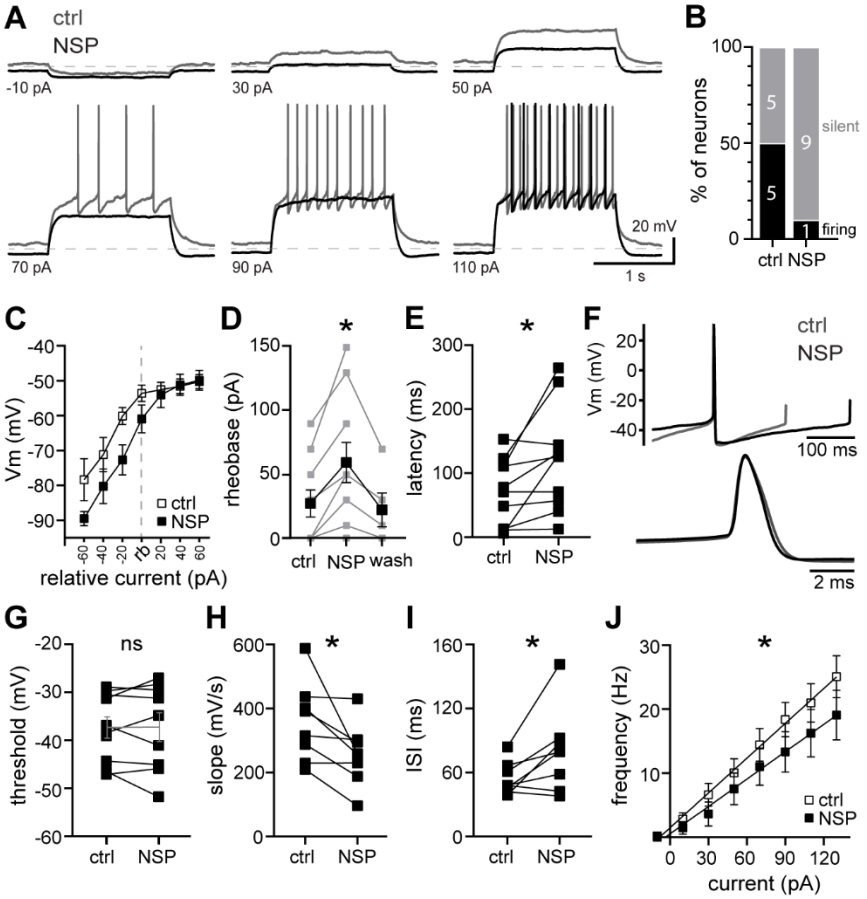

Figure 4. Tonic GluD1$_R$ current provides subthreshold drive of action potential firing. (**A**) Representative traces of whole-cell current clamp recordings of membrane potential and AP firing evoked by current injection (1.5 s) demonstrating hyperpolarization by NASPM. Dashed line is at -80 mV. (**B**) Distribution of firing response in control (ctrl) and after application of NASPM (NSP). In control conditions 5/10 neurons fired spontaneously without current injection and 5/10 were silent. In the same neurons after NASPM, 1/10 fired spontaneously and 9/10 were silent. (**C**) Plot of the membrane potential (Vm) versus injected current relative to rheobase (rb) in control (open squares) and NASPM (closed squares), demonstrating that NASPM produced a hyperpolarization at subthreshold potentials. Membrane potential during AP firing was measured as the average interspike Vm. (**D**) Plot of the minimum current needed to induce firing (approximate rheobase) in control conditions, NASPM, and following wash out of NASPM (10 min) ($p = 0.005$, $n = 5$-10). (**E**) NASPM increased the latency to fire the first AP upon current injection (150 pA, $p = 0.01$, $n = 10$). (**F**) Average AP waveform recorded in control and in NASPM, aligned at peaks. Below, expanded timescale. (**G**) NASPM had no effect on the AP threshold (150 pA, measured from the 2nd AP, $p < 0.99$, $n = 9$). (**H**) NASPM decreased the slope of the voltage trajectory between APs (90 pA, measured in the middle 60% of the interspike interval of the first 5 APs, $p = 0.02$, $n = 8$). (**I**) NASPM increased the interspike interval during evoked firing (90 pA, averaged from first 5 APs, $p = 0.04$, $n = 8$). (**J**) Plot of the initial firing frequency (first 3 APs) versus injected current in control (open squares) and NASPM (closed squares). Line and error bars represent mean ± SEM. * denotes statistical significance, ns denotes not significant.

REFERENCES

Ady V, Perroy J, Tricoire L, Piochon C, Dadak S, Chen X, Dusart I, Fagni L, Lambolez B, Levenes C. 2013. Type 1 metabotropic glutamate receptors (mGlu1) trigger the gating of GluD2 delta glutamate receptors. *EMBO rep* 15:103–109. doi:10.1002/embr.201337371

Araki K, Meguro H, Kushiya E, Takayama C, Inoue Y, Mishina M. 1993. Selective expression of the glutamate receptor channel delta 2 subunit in cerebellar Purkinje cells. *Biochem Biophys Res Commun* 197:1267–1276. doi:10.1006/bbrc.1993.2614

Baraban JM, Wang RY, Aghajanian G. 1978. Reserpine suppression of dorsal raphe neuronal firing: mediation by adrenergic system. *Eur J Pharmacol* 52:27–36.

Benamer N, Marti F, Luján R, Hepp R, Aubier TG, Dupin AAM, Frébourg G, Pons S, Maskos U, Faure P, Hay YA, Lambolez B, Tricoire L. 2018. GluD1, linked to schizophrenia, controls the burst firing of dopamine neurons. *Mol Psychiatry* 23:691–700. doi:10.1038/mp.2017.137

Bond RA, IJzerman AP. 2006. Recent developments in constitutive receptor activity and inverse agonism, and their potential for GPCR drug discovery. *Trends Pharmacol Sci* 27:92–96. doi:10.1016/j.tips.2005.12.007

Brown RE, Sergeeva OA, Eriksson KS, Haas HL. 2002. Convergent excitation of dorsal raphe serotonin neurons by multiple arousal systems (orexin/hypocretin, histamine and noradrenaline). *Journal of Neuroscience* 22:8850–8859. doi:10.1523/jneurosci.22-20-08850.2002

Dadak S, Bouquier N, Goyet E, Fagni L, Levenes C, Perroy J. 2017. mGlu1 receptor canonical signaling pathway contributes to the opening of the orphan GluD2 receptor. *Neuropharmacology* 115:92–99. doi:10.1016/j.neuropharm.2016.06.001

Dai J, Patzke C, Liakath-Ali K, Seigneur E, dhof TCS x000FC. 2021. GluD1 is a signal transduction device disguised as an ionotropic receptor. *Nature* 1–21. doi:10.1038/s41586-021-03661-6

Eggermann E, Bucurenciu I, Goswami SP, Jonas P. 2011. Nanodomain coupling between Ca2+ channels and sensors of exocytosis at fast mammalian synapses. *Nat Rev Neurosci* 13:7–21. doi:10.1038/nrn3125

Egorov AV, Hamam BN, Fransén E, Hasselmo ME, Alonso AA. 2002. Graded persistent activity in entorhinal cortex neurons. *Nature* 420:173–178. doi:10.1038/nature01171

Egorov AV, Schumacher D, Medert R, Birnbaumer L, Freichel M, Draguhn A. 2019. TRPC channels are not required for graded persistent activity in entorhinal cortex neurons. *Hippocampus* 29:1038–1048. doi:10.1002/hipo.23094

Fossati M, Assendorp N, Gemin O, Colasse S, Dingli F, Arras G, Loew D, Charrier C. 2019. Trans-Synaptic Signaling through the Glutamate Receptor Delta-1 Mediates Inhibitory Synapse Formation in Cortical Pyramidal Neurons. *Neuron* 104:1081-1094.e7. doi:10.1016/j.neuron.2019.09.027

316 Gantz SC, Bunzow JR, Williams JT. 2013. Spontaneous inhibitory synaptic currents mediated by a G protein-coupled
317 receptor. *Neuron* 78:807–812. doi:10.1016/j.neuron.2013.04.013

318 Gantz SC, Moussawi K, Hake HS. 2020. Delta glutamate receptor conductance drives excitation of mouse dorsal
319 raphe neurons. *Elife* 9:103. doi:10.7554/elife.56054

320 Gawande DY, Shelkar GP, Liu J, Ayala AD, Pavuluri R, Choi D, Smith Y, Dravid SM. 2021. Glutamate Delta-1 Receptor
321 Regulates Inhibitory Neurotransmission in the Nucleus Accumbens Core and Anxiety-Like Behaviors. *Mol*
322 *Neurobiol* 1–15. doi:10.1007/s12035-021-02461-3

323 Hein P, Goepel M, Cotecchia S, Michel MC. 2001. A quantitative analysis of antagonism and inverse agonism at wild-
324 type and constitutively active hamster α1B-adrenoceptors. *Naunyn-schmiedeberg's Archives Pharmacol* 363:34–
325 39. doi:10.1007/s002100000329

326 Hepp R, Hay YA, Aguado C, Luján R, Dauphinot L, Potier MC, Nomura S, Poirel O, Mestikawy SE, Lambolez B,
327 Tricoire L. 2015. Glutamate receptors of the delta family are widely expressed in the adult brain. *Brain Struct*
328 *Funct* 220:2797–2815. doi:10.1007/s00429-014-0827-4

329 Jackson AC, Yao GL, Bean BP. 2004. Mechanism of spontaneous firing in dorsomedial suprachiasmatic nucleus
330 neurons. *Journal of Neuroscience* 24:7985–7998. doi:10.1523/jneurosci.2146-04.2004

331 Khaliq ZM, Bean BP. 2010. Pacemaking in dopaminergic ventral tegmental area neurons: depolarizing drive from
332 background and voltage-dependent sodium conductances. *Journal of Neuroscience* 30:7401–7413.
333 doi:10.1523/jneurosci.0143-10.2010

334 Khamma JK, Copeland DS, Hake HS, Gantz SC. 2021. Spatiotemporal control of noradrenaline-dependent synaptic
335 transmission in mouse dorsal raphe serotonin neurons. *Journal of Neuroscience* JN-RM-1176-21.
336 doi:10.1523/jneurosci.1176-21.2021

337 Koike M, Iino M, Ozawa S. 1997. Blocking effect of 1-naphthyl acetyl spermine on Ca(2+)-permeable AMPA
338 receptors in cultured rat hippocampal neurons. *Neuroscience Research* 29:27–36. doi:10.1016/s0168-
339 0102(97)00067-9

340 Konno K, Matsuda K, Nakamoto C, Uchigashima M, Miyazaki T, Yamasaki M, Sakimura K, Yuzaki M, Watanabe M.
341 2014. Enriched expression of GluD1 in higher brain regions and its involvement in parallel fiber-interneuron
342 synapse formation in the cerebellum. *Journal of Neuroscience* 34:7412–7424. doi:10.1523/jneurosci.0628-
343 14.2014

344 Kramer PF, Williams JT. 2016. Calcium Release from Stores Inhibits GIRK. *Cell Reports* 17:3246–3255.
345 doi:10.1016/j.celrep.2016.11.076

346 Lemoine D, Mondoloni S, Tange J, Lambolez B, Faure P, Taly A, Tricoire L, Mourot A. 2020. Probing the ionotropic
347 activity of glutamate GluD2 receptor in HEK cells with genetically-engineered photopharmacology. *Elife* 9:103.
348 doi:10.7554/elife.59026

349 Li K, Abbott SBG, Shi Y, Eggan P, Gonye EC, Bayliss DA. 2021. TRPM4 mediates a subthreshold membrane potential
350 oscillation in respiratory chemoreceptor neurons that drives pacemaker firing and breathing. *Cell Reports*
351 34:108714–108714. doi:10.1016/j.celrep.2021.108714

Lomeli H, Sprengel R, Laurie DJ, Kohr G, Herb A, Seeburg PH, Wisden W. 1993. The rat delta-1 and delta-2 subunits extend the excitatory amino acid receptor family. *FEBS Letters* 315:318–322. doi:10.1016/0014-5793(93)81186-4

Loucif AJC, Bonnavion P, Macri B, Golmard J-L, Boni C, Melfort M, Leonard G, Lesch K-P, Adrien J, Jacquin TD. 2006. Gender-dependent regulation of G-protein-gated inwardly rectifying potassium current in dorsal raphe neurons in knock-out mice devoid of the 5-hydroxytryptamine transporter. *J Neurobiol* 66:1475–1488. doi:10.1002/neu.20321

Lu B, Su Y, Das S, Liu J, Xia J, Ren D. 2007. The neuronal channel NALCN contributes resting sodium permeability and is required for normal respiratory rhythm. *Cell* 129:371–383. doi:10.1016/j.cell.2007.02.041

Lu B, Zhang Q, Wang H, Wang Y, Nakayama M, Ren D. 2010. Extracellular Calcium Controls Background Current and Neuronal Excitability via an UNC79-UNC80-NALCN Cation Channel Complex. *Neuron* 68:488–499. doi:10.1016/j.neuron.2010.09.014

Nakamoto C, Konno K, Miyazaki T, Nakatsukasa E, Natsume R, Abe M, Kawamura M, Fukazawa Y, Shigemoto R, Yamasaki M, Sakimura K, Watanabe M. 2020. Expression mapping, quantification, and complex formation of GluD1 and GluD2 glutamate receptors in adult mouse brain. *J Comp Neurol* 528:1003–1027. doi:10.1002/cne.24792

Pfaffinger PJ, Martin JM, Hunter DD, Nathanson NM, Hille B. 1985. GTP-binding proteins couple cardiac muscarinic receptors to a K channel. *Nature* 317:536–538. doi:10.1038/317536a0

Philippart F, Khaliq ZM. 2018. Gi/o protein-coupled receptors in dopamine neurons inhibit the sodium leak channel NALCN. *Elife* 7:1. doi:10.7554/elife.40984

Prézeau L, Gomeza J, Ahern S, Mary S, Galvez T, Bockaert J, Pin JP. 1996. Changes in the carboxyl-terminal domain of metabotropic glutamate receptor 1 by alternative splicing generate receptors with differing agonist-independent activity. *Mol Pharmacol* 49:422–9.

Quallo T, Alkhatib O, Gentry C, Andersson DA, Bevan S. 2017. G protein βγ subunits inhibit TRPM3 ion channels in sensory neurons. *Elife* 6:870. doi:10.7554/elife.26138

Raman IM, Gustafson AE, Padgett D. 2000. Ionic currents and spontaneous firing in neurons isolated from the cerebellar nuclei. *Journal of Neuroscience* 20:9004–16.

Rodriguez-Contreras D, Condon AF, Buck DC, Asad N, Dore TM, Verbeek DS, Tijssen MAJ, Shinde U, Williams JT, Neve KA. 2021. Signaling-Biased and Constitutively Active Dopamine D2 Receptor Variant. *Acs Chem Neurosci* 12:1873–1884. doi:10.1021/acschemneuro.0c00712

Shen Y, Rampino MAF, Carroll RC, Nawy S. 2012. G-protein-mediated inhibition of the Trp channel TRPM1 requires the G dimer. *Proc National Acad Sci* 109:8752–8757. doi:10.1073/pnas.1117433109

Svensson TH, Bunney BS, Aghajanian GK. 1975. Inhibition of both noradrenergic and serotonergic neurons in brain by the alpha-adrenergic agonist clonidine. *Brain Res* 92:291–306. doi:10.1016/0006-8993(75)90276-0

Taddese A, Bean BP. 2002. Subthreshold Sodium Current from Rapidly Inactivating Sodium Channels Drives Spontaneous Firing of Tuberomammillary Neurons. *Neuron* 33:587–600. doi:10.1016/s0896-6273(02)00574-3

388 Tao W, Díaz-Alonso J, Sheng N, Nicoll RA. 2018. Postsynaptic δ1 glutamate receptor assembles and maintains
389 hippocampal synapses via Cbln2 and neurexin. *Proceedings of the National Academy of Sciences* 115:E5373–
390 E5381. doi:10.1073/pnas.1802737115

391 Top M van den, Lee K, Whyment AD, Blanks AM, Spanswick D. 2004. Orexigen-sensitive NPY/AgRP pacemaker
392 neurons in the hypothalamic arcuate nucleus. *Nat Neurosci* 7:493–494. doi:10.1038/nn1226

393 Vandermaelen CP, Aghajanian GK. 1983. Electrophysiological and pharmacological characterization of serotonergic
394 dorsal raphe neurons recorded extracellularly and intracellularly in rat brain slices. *Brain Res* 289:109–119.
395 doi:10.1016/0006-8993(83)90011-2

396 Yamada-Hanff J, Bean BP. 2013. Persistent sodium current drives conditional pacemaking in CA1 pyramidal
397 neurons under muscarinic stimulation. *Journal of Neuroscience* 33:15011–15021. doi:10.1523/jneurosci.0577-
398 13.2013

399 Yuzaki M, Aricescu AR. 2017. A GluD Coming-Of-Age Story. *Trends Neurosci* 40:138–150.
400 doi:10.1016/j.tins.2016.12.004

401 Zhang X, Mak S, Li L, Parra A, Denlinger B, Belmonte C, McNaughton PA. 2012. Direct inhibition of the cold-
402 activated TRPM8 ion channel by Gαq. *Nat Cell Biol* 14:851–858. doi:10.1038/ncb2529

403